

Intrinsic noise properties of atomic point contact displacement detectors

N. E. Flowers-Jacobs,^{1,2,*} D. R. Schmidt,^{1,2} and K. W. Lehnert^{1,2}

¹*JILA, National Institute of Standards and Technology and the University of Colorado, Boulder, CO 80309, USA*

²*Department of Physics, University of Colorado, Boulder, CO 80309, USA*

We measure the noise added by an atomic point contact operated as a displacement detector. With a microwave technique, we increase the measurement speed of atomic point contacts by a factor of 500. The measurement is then fast enough to detect the resonant motion of a nanomechanical beam at frequencies up to 60 MHz and sensitive enough to observe the random thermal motion of the beam at 250 mK. We demonstrate a shot-noise limited imprecision of 2.3 ± 0.1 fm/ $\sqrt{\text{Hz}}$ and observe a 78 ± 20 aN/ $\sqrt{\text{Hz}}$ backaction force, yielding a total uncertainty in the beam's displacement that is 42 ± 9 times the standard quantum limit.

PACS numbers: 73.40.Gk, 85.85.+j, 73.23.-b, 72.70.+m

Both to realize quantum-limited measurement of position and to develop ultrasensitive detectors, there has been a renewed effort to more precisely measure the motion of nanomechanical elements. Recent examples include the demonstration of near quantum limited displacement sensitivity using single electron transistors [1, 2] as well as novel sensors of nanomechanical motion that use mesoscopic strain gauges in the form of carbon nanotubes[3] or quantum point contacts [4]. There has been a parallel development in theories that calculate the noise properties of these sensors [5, 6, 7, 8, 9, 10], focusing on how closely they can approach displacement measurement at the standard quantum limit [10, 11]. Reaching the standard quantum limit is a compromise between minimizing the purely apparent motion of the nanomechanical element inferred from noise at the output of the sensor, that is, the displacement imprecision $S_x(\omega)$, and minimizing the real random motion caused by the sensor, described as a backaction force with spectral density $S_F(\omega)$. A continuous linear measurement of position is subject to the Heisenberg constraint $\sqrt{S_x S_F} \geq \hbar$, Ref. [12]. When measuring the position of a harmonic oscillator, the standard quantum limit is most closely approached when $S_x(\omega) = |H(\omega)|^2 S_F(\omega)$ assuming $S_x(\omega)$ and $S_F(\omega)$ are uncorrelated, where $H(\omega)$ is the harmonic oscillator's response function [10, 11].

A displacement detector based on electrons tunneling from an atomic point contact (APC) has three attributes that make it a promising amplifier of nanomechanical motion. First, the intrinsic noise at the output of the atomic point contact, electrical shot-noise, can easily overwhelm the noise at the input of conventional amplifiers. This is a crucial prerequisite for quantum-limited amplification. Second, the APC need not be operated at ultralow temperatures. Both advantages arise from the relatively large energy scale, the few electron-volt work function of the metal, that controls electron tunneling in the APC. Finally, recent theoretical work [5, 7, 8, 10, 13] has predicted that a displacement detector based on an APC would be a quantum mechanically ideal amplifier. In addition, the atomic point contact is already an impor-

tant and commonly used displacement detector as it provides the exceptional spatial resolution in scanning tunneling microscopes and mechanically adjustable break-junctions. Until now, the atomic point contact neither has been operated with sufficient temporal resolution to sense a nanomechanical element moving at its resonance frequency nor has its backaction been measured.

In this Letter, we measure the intrinsic noise of a displacement sensor based on an atomic point contact, finding both its imprecision S_x and backaction S_F spectral densities. As in scanning tunneling microscopy, we infer the distance between an atomically sharp point and a nearby conducting object from the tunneling resistance across the APC. However, by detecting the APC's resistance at microwave frequencies we can measure displacement on times less than 10 nanoseconds. The measurement is fast and sensitive enough to resolve the submicrosecond, subpicometer resonant motion of a nanomechanical beam driven by thermal noise at temperatures below 1 K. The random thermal motion of the nanomechanical beam provides a calibrated noise source which can be used to determine the displacement imprecision and backaction of the APC. Our current realization of this displacement detector, an APC amplifier, has a displacement imprecision $\sqrt{S_x} = 2.3 \pm 0.1$ fm/ $\sqrt{\text{Hz}}$ and a backaction $\sqrt{S_F} = 78 \pm 20$ aN/ $\sqrt{\text{Hz}}$ yielding a total displacement uncertainty that is 42 times the standard quantum limit and an imprecision-backaction product $\sqrt{S_x S_F} = 1700 \pm 400 \hbar$. We demonstrate that the imprecision of our measurement is shot-noise limited; however, we also observe that the backaction force is much larger than theoretically predicted.

An APC is formed by bringing an atomically sharp conducting point within 1 nm of another conducting object [14]. To monitor the size of the gap between the point and the other object [Fig. 1(a)], a voltage bias is applied across the gap and the probability of electron tunneling is determined by measuring the current. The ratio of the voltage V to the average current $\langle I \rangle$ is a resistance R that changes monotonically with the size of the gap. The APC can then be regarded as both a trans-

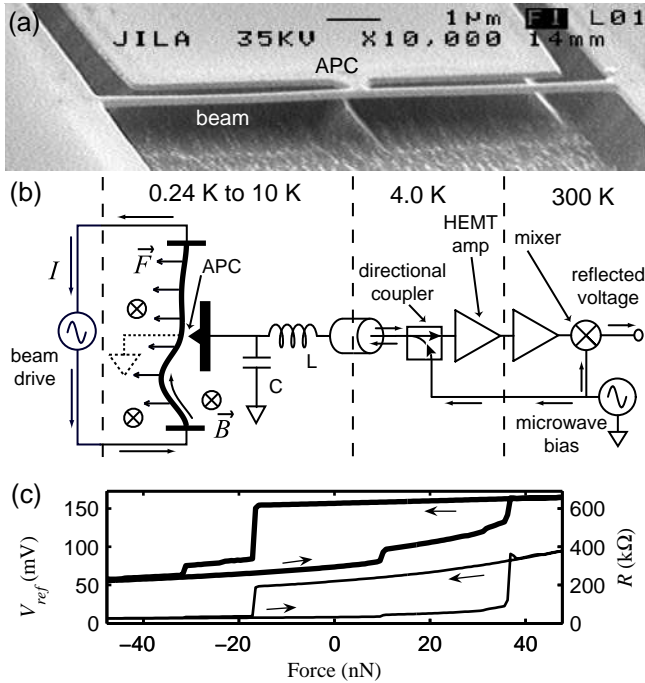


FIG. 1: (a) Representative scanning electron micrograph of the nanomechanical system consisting of a doubly clamped beam suspended above a GaAs substrate and a triangular electrode fused to the beam center; the APC is formed at the junction between the electrode and the beam. (b) Simplified schematic consisting of a displacement measurement shown to the right of the APC and a drive mechanism (using a Lorentz force created by passing a current through the beam in the presence of a 9 T magnetic field) shown to the left. (c) V_{ref} (thick line) and APC resistance (thin line, measured at 7 Hz using a lock-in amplifier) versus static applied Lorentz force. We observe a monotonic relationship between R and V_{ref} .

ducer and an amplifier of small displacements dx with an output $d\langle I \rangle = G dx$, where $G = (1/R)(\partial R/\partial x)\langle I \rangle$ is the amplifier's gain.

Only a small fraction of an APC's intrinsically large bandwidth is typically realized because the APC is also necessarily a high-resistance device [14]. The high resistance shunted by the large cable capacitance between the device and the remote measurement electronics [15] creates an approximately 100 kHz bandwidth limit. We overcome this bandwidth limitation by transforming down the resistance of the APC towards 50Ω with an electrical resonant transformer formed out of an inductor L and capacitor C , inferring the resistance by measuring the on-resonance ($1/2\pi\sqrt{LC} = 430$ MHz) reflected microwave voltage V_{ref} [Fig. 1(b,c)], where $\langle I \rangle$ is now the magnitude of the *microwave* current passing through the APC. With this technique, originally implemented in the radio-frequency single-electron transistor[15], we achieve a bandwidth of 30 MHz controlled by the quality factor of the resonant circuit; it is possible to detect motion out-

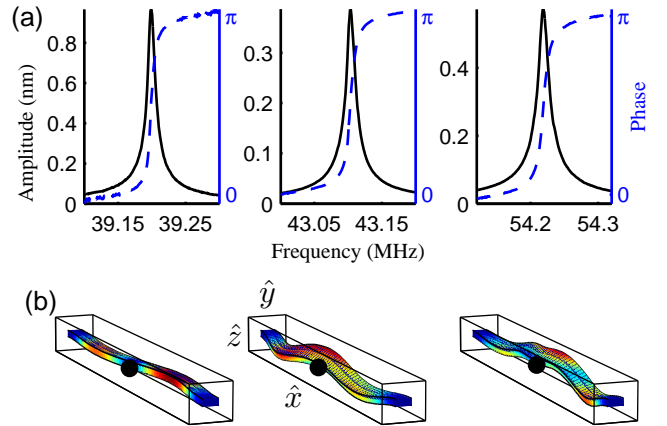


FIG. 2: (Color online) (a) Measured response amplitude (solid) and phase (dashed) as a function of drive frequency for three of the five observed resonant modes measured with the APC amplifier. (b) Corresponding finite-element simulation of beam mode shapes (dot corresponds to position of spring used to model the interatomic potential at the APC; color indicates displacement from equilibrium position with minimum displacement at the ends of the beam).

side of this band at the cost of a larger contribution to the measurement noise by the conventional electronics. Further increases in the bandwidth are possible by using higher-frequency resonant circuits. We choose to operate the APC amplifier with a 430 MHz resonance frequency because low-noise microwave amplifiers are readily available at this frequency, and the resonant circuit can be fabricated from discrete components.

The mechanical system in this experiment is composed of a doubly clamped nanomechanical beam next to an atomically sharp point [Fig. 1(a)]. The beam and point electrode are made entirely out of gold and are fabricated fused together. An APC is formed between the point and the beam by creating a gap using electromigration[16] in the ultrahigh vacuum present in a 4 K cryostat; despite this precaution, it is still possible that contaminants in the gap between the beam and the point play a role in this experiment. The beam is $5.6\text{-}\mu\text{m}$ long by 220-nm wide by 100-nm thick resulting in a total beam mass $m = 2.3 \times 10^{-15}$ kg.

We demonstrate the bandwidth of the APC amplifier by finding the resonant frequencies of the beam. These resonant modes are detected by sweeping the frequency of an oscillating 50 pN Lorentz force [Fig. 1(b)] applied to the beam parallel to the substrate (\hat{y} direction, [Fig. 2(b)]) and using the APC amplifier to look for resonances[17]. We observe five resonance frequencies between $\omega_0/2\pi = 18.4$ MHz and 57.2 MHz with a typical quality factor of 5000 [Fig. 2(a)]. An interatomic potential between the gold atoms comprising the APC modifies the resonance frequencies and mode shapes from those expected for a doubly clamped beam. While for large

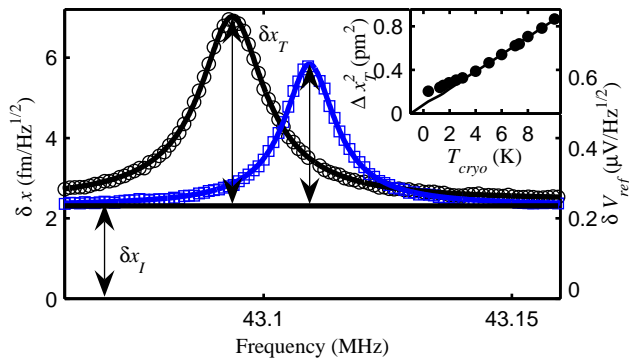


FIG. 3: (Color online) (Main) APC amplifier noise spectrum δV_{ref} (right axis) versus frequency and corresponding displacement fluctuations of the beam δx (left axis) at 5 K (squares, right peak) and 10 K (circles, left peak) and square root of Lorentzian fits (lines); the noise spectra were measured with an APC resistance of 33 k Ω , and for this $G = 290$ nA/nm the microwave voltage across the APC was 26 mV. (Inset) Integrated strength Δx_T^2 as a function of T_{cryo} (dot, $G = 290$ nA/nm) with a fit (line) to the model for Δx_T^2 . For low temperatures we observe deviations from the model due to locally heating by the bias current of the dissipative environment coupled to the mechanical system.

static applied forces there is hysteresis in the beam's displacement [Fig. 1(c)], for small displacements from mechanical equilibrium the net effect of the interatomic potential deflecting the beam can be modeled as a spring spanning the APC, which connects the point and the beam. In a finite element simulation, we adjust the compliance of the spring until the simulated resonance frequencies match those observed. Although this 180 N/m spring results in simulated mode shapes that appear complicated [Fig. 2(b)], near a resonance frequency the system behaves like a one-dimensional simple harmonic oscillator [17] with a collective coordinate whose displacement is equal to the root-mean-squared displacement of the beam averaged over the beam's length [Fig. 2(a)]. Because we specify displacement exclusively in terms of this normal (or modal) coordinate, the effective spring constant of the simple harmonic oscillator is $k_s = m\omega_0^2$ with m equal to the *total* mass of the beam.

To characterize the displacement imprecision and amplifier backaction in our measurement, we find the noise spectrum δV_{ref} when the beam is not driven by a Lorentz force [Fig. 3(main)]. The noise spectrum has two components, a frequency independent background and Lorentzian peaks at the beam's mechanical resonance frequencies due to the Brownian motion of the beam. We calibrate δV_{ref} in displacement units through the temperature dependence of the Brownian motion. Through this ratio of V_{ref} and x and through the relationship between V_{ref} and R in [Fig. 1(c)], we find $(1/R)(\partial R/\partial x) = 0.4$ nm $^{-1}$ when $R = 33$ k Ω , the operating point where we observe minimum imprecision. From

a fit to the Lorentzian peak we extract the full width of the peak at half maximum $\gamma/2\pi$ (defined so that the harmonic oscillator feels a dissipative force $m\gamma(\partial x/\partial t)$), center frequency $\omega_0/2\pi$, amplitude δx_T , and frequency-independent background $\delta x_I = \sqrt{S_x}$. These fit values are used to calculate the integrated strength of the Lorentzian peak $\Delta x_T^2 = \delta x_T^2 \gamma/4$ as a function of the cryostat's temperature T_{cryo} [Fig. 3(inset)]. While the equipartition theorem predicts $\Delta x_T^2 = k_B T_{cryo}/k_s$, we model $\Delta x_T^2 = (k_B T_{cryo}/k_s) + (S_F/4m\gamma k_s)$, where the spectral density of a random force S_F depends upon G (which is equivalent to depending on the amplitude of the microwave bias current). From this dependence, we infer that the measurement process imposes a random force S_F effectively heating the beam to a temperature $T_{BA} = S_F/4m\gamma k_B$ above T_{cryo} [Fig. 4a]. While we model S_F as independent of T_{cryo} , T_{BA} has a T_{cryo} dependence through γ , which changes by 30% in the 0.25 K to 10 K range of T_{cryo} . For the maximum gain $G = 290$ nA/nm studied and $\omega_0/2\pi = 43.1$ MHz, we measure both the minimum imprecision $\sqrt{S_x} = 2.3 \pm 0.1$ fm/ $\sqrt{\text{Hz}}$ and the maximum random force $\sqrt{S_F} = 78 \pm 20$ aN/ $\sqrt{\text{Hz}}$ acting on the beam; this random force implies that at $T_{cryo} = 5$ K there is a backaction temperature $T_{BA} = 0.73 \pm 0.4$ K.

We compare these results to limits imposed by the Heisenberg uncertainty principle. A Heisenberg limited amplifier with gain chosen to operate at the standard quantum limit would have an imprecision $S_x^{SQL} = \hbar|H(\omega)|$ and a backaction force $S_F^{SQL} = \hbar/|H(\omega)|$, where $H(\omega) = 1/m(\omega_0^2 - \omega^2 + i\omega\gamma)$ is the beam's response function [10, 11, 17]. On resonance, $\sqrt{S_x^{SQL}} = \sqrt{\hbar/m\omega_0\gamma} = 51$ am/ $\sqrt{\text{Hz}}$ and $\sqrt{S_F^{SQL}} = \sqrt{\hbar m\omega_0\gamma} = 2.1$ aN/ $\sqrt{\text{Hz}}$. Comparing to these, we find that for our APC amplifier $\sqrt{S_x} = 45 \sqrt{S_x^{SQL}}$ and $\sqrt{S_F} = 38 \sqrt{S_F^{SQL}}$. By assuming that the fluctuations imposed by the random backaction force are uncorrelated with the measurement imprecision, we make a worst case estimate of the quantum nonideality of the APC as a displacement amplifier. We find that $\sqrt{S_x S_F} = 1700 \pm 400 \hbar$, which is 1700 times the Heisenberg-limited imprecision-backaction product. As with most amplifiers, the APC amplifier imprecision can be reduced by increasing G at the expense of a larger backaction [10, 11] [Fig. 4(b)]. We have therefore operated the APC amplifier near an optimum G that minimizes the *total* displacement uncertainty on resonance $\sqrt{S_x^{tot}} = \sqrt{S_x + S_F|H(\omega_0)|^2} = 42 \pm 9 \sqrt{2\hbar/m\omega_0\gamma}$, i.e., 42 times the total displacement uncertainty at the standard quantum limit [Fig. 4].

Because the physical origins of the imprecision and backaction that combine to enforce the Heisenberg limit in the theoretical treatment of an APC amplifier are readily understood [7, 8], we can speculate about the source of the nonideality in our APC amplifier. The fundamental imprecision in the APC is electrical shot noise; that

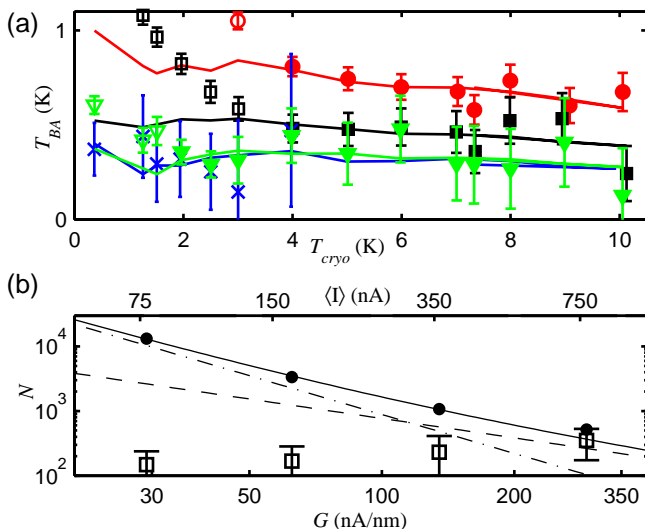


FIG. 4: (Color online) (a) Backaction temperature T_{BA} versus the temperature of the cryogenic system, T_{cryo} , with gains $G=290$ nA/nm (circle), $G=130$ nA/nm (square), $G=60$ nA/nm (triangle), and $G=30$ nA/nm (cross). Error bars are extracted from one sigma uncertainties in fits to Lorentzian noise peaks [Fig. 3]; hollow symbols are excluded from the fit (lines) to the model. (b) Measurement imprecision quanta $N_x = k_s S_x \gamma / 4 \hbar \omega_0$ (solid dots) and momentum backaction quanta $N_p = S_F / 4 m \gamma \hbar \omega_0$ (hollow squares) at 5 K as a function of G . The uncertainty in the imprecision (error bars are the size of the solid dots) and backaction are dominated by the uncertainty in the beam temperature. As G is increased by increasing the average current $\langle I \rangle$, the compromise between a reduced imprecision and increased backaction is evident. At the maximum G the imprecision is determined by the intrinsic noise S_I^{SN} of the APC amplifier $N_{SN} = k_s S_I^{SN} \gamma / 4 G^2 \hbar \omega_0$ (dashed line). For smaller values of G , the imprecision is dominated by noise S_I^A added by the HEMT microwave amplifier $N_A = k_s S_I^A \gamma / 4 G^2 \hbar \omega_0$ (dot-dashed line), [Fig. 1(c)]. The measurement imprecision is the sum of these two contribution $N_x = N_{SN} + N_A$ (solid line).

is, random Poissonian fluctuations in the electron tunneling rate [7, 13]. Similarly, the backaction that enforces the Heisenberg limit is due to the random magnitude of the momentum kicks imparted to the beam by each electron that tunnels [8]. To realize an ideal quantum amplifier, these sources of imprecision and backaction must dominate. In contrast to single-electron transistor and quantum point contact displacement detection [1, 2, 4], it is relatively easy to ensure that the noise power S_I^A added by conventional amplifiers and electrical components [Fig. 1(b)] is overwhelmed by the shot noise of tunneling electrons $S_I^{SN} = 2e \langle I \rangle (2\sqrt{2}/\pi)$, where the $2\sqrt{2}/\pi$ factor arises from averaging the instantaneous shot noise over one cycle of the microwave bias. Indeed we find that for the $G=290$ nA/nm, the maximum gain studied, the electrical shot noise accounts for 70% of the spectral density of the displacement imprecision and only 30% comes from the rest of the measurement circuit [Fig. 4(b)].

In spite of the fact that the imprecision is shot-noise limited, it is still substantially larger than was estimated by [7]. It is through a smaller value of $\partial R / \partial x$ that the gain G at a particular current value is smaller and the shot-noise limited imprecision $S_x = S_I^{SN} / G^2$ is larger than predicted. Assuming the APC resistance obeys $R = R_0 \exp(2\alpha x / \lambda)$, the usual one-dimensional model for electron tunneling [18], where $\lambda = 90$ pm in gold and $\alpha = 0.4 \pm 0.2$ is a mode dependent factor relating normal coordinate displacement x to displacement at the APC, then $\sqrt{S_x}$ should be $70 \text{ am} / \sqrt{\text{Hz}}$ at the highest experimental bias current. However, in our experiment we infer from $\partial R / \partial x$ that $\lambda = 2 \pm 1 \text{ nm}$ resulting in a shot-noise limited imprecision $\sqrt{S_x} = 2 \pm 1 \text{ fm} / \sqrt{\text{Hz}}$. Despite known deviations from the simple exponential dependence of resistance on position for tunnel resistances R_0 less than $1 \text{ M}\Omega$ [19], we operate at resistances less than $100 \text{ k}\Omega$ so that the imprecision, displacement due to backaction, and thermal motion (at temperatures where the bias heating can be ignored) are all approximately equal.

Since the imprecision is shot-noise limited, we conclude that the likely source of nonideality in our APC amplifier is a backaction in excess of the backaction required by the Heisenberg uncertainty principle. Two sources of excess backaction force on the nanomechanical beam were considered by [20]. First, shot noise in the mean momentum of the tunneling electrons results in a backaction force. Second, an electrostatic attraction between the beam and the APC creates a backaction force through a mutual capacitance and a fluctuating voltage across the APC. We do not yet understand the origin of the excess backaction; however, to account for the observed backaction the mean momentum $\langle p \rangle$ imparted by each tunneling electron would have to be $\langle p \rangle = e \sqrt{S_F / S_I^{SN}} = 20$ times the Fermi momentum, while the capacitive mechanism predicts a cubic dependence [7] of S_F on gain G , apparently inconsistent with the observed dependence [Fig. 4b].

In conclusion, we have demonstrated a method of using an APC to measure displacement. We increase the electrical bandwidth (the measurement speed) of the APC and use this bandwidth to sensitively detect the motion of a nanomechanical beam at frequencies up to 60 MHz. We observe the imprecision and backaction to set an upper limit on the nonideality of an APC as a quantum amplifier, yielding an imprecision-backaction product of $\sqrt{S_x S_F} = 1700 \hbar$ and a total displacement uncertainty of 42 times the standard-quantum limit. Since the imprecision of the APC amplifier is limited by its fundamental noise source, the shot-noise of tunneling electrons, progress towards the quantum limit will not require an improvement in the performance of conventional electronics but rather an understanding of the excess backaction.

The authors acknowledge support from the National Science Foundation under grant number PHY0096822 and the National Institute of Standards and Technology. The authors also wish to thank J. G. E. Harris, A. A. Clerk, S. M. Girvin, R. Mirin, and C. T. Rogers for enlightening conversations and technical assistance.

-
- * Electronic address: nathan.flowers-jacobs@colorado.edu
- [1] R. G. Knobel and A. N. Cleland, *Nature* **424**, 291 (2003).
 - [2] M. D. LaHaye *et al.*, *Science* **304**, 74 (2004).
 - [3] V. Sazonova *et al.*, *Nature* **431**, 284 (2004).
 - [4] A. N. Cleland *et al.*, *Appl. Phys. Lett.* **81**, 1699 (2002).
 - [5] D. Mozyrsky and I. Martin, *Phys. Rev. Lett.* **89**, 018301 (2002).
 - [6] D. Mozyrsky, I. Martin, and M. B. Hastings, *Phys. Rev. Lett.* **92**, 018303 (2004).
 - [7] M. F. Bocko, K. A. Stephenson, and R. H. Koch, *Phys. Rev. Lett.* **61**, 726 (1988).
 - [8] B. Yurke and G. P. Kochanski, *Phys. Rev. B* **41**, 8184

- (1990).
- [9] M. P. Blencowe and M. N. Wybourne, *Appl. Phys. Lett.* **77**, 3845 (2000).
- [10] A. A. Clerk, *Phys. Rev. B* **70**, 245306 (2004).
- [11] C. M. Caves, *Phys. Rev. D* **26**, 1817 (1982).
- [12] Refs. [10, 11] state $S_x S_F \geq \hbar^2/4$. This difference arises from our use of a one-sided spectral density, e.g., $S_x(f) = 2 \int_0^\infty dt \langle x(t)x(0) \rangle e^{i2\pi f t}$, instead of the two-sided spectral density used in Refs. [10, 11].
- [13] A. A. Clerk and S. M. Girvin, *Phys. Rev. B* **70**, 121303(R) (2004).
- [14] N. Agraït, A. L. Yeyati, and J. M. van Ruitenbeek, *Phys. Rep.* **377**, 81 (2003).
- [15] R. J. Schoelkopf *et al.*, *Science* **280**, 1238 (1998).
- [16] H. Park *et al.*, *Appl. Phys. Lett.* **75**, 301 (1999).
- [17] K. L. Ekinci and M. L. Roukes, *Rev. Sci. Instrum.* **76**, 061101 (2005).
- [18] J. G. Simmons, *J. Appl. Phys.* **34**, 1793 (1963).
- [19] Y. Sun *et al.*, *Phys. Rev. B* **71**, 193407 (2005).
- [20] K. A. Stephenson, M. F. Bocko, and R. H. Koch, *Phys. Rev. A* **40**, 6615 (1989).